Transient analysis of the slamming wave load on an offshore wind turbine foundation generated by different types of breaking waves

Ahmad Darori Hasan[1], Yu-Hsien Lin[1*]
[1]*Dept. of Systems & Naval Mechatronic Eng., National Cheng-Kung University, Tainan City 70101, Taiwan*
**Email: vyhlin@mail.ncku.edu.tw*

Abstract

In this study, a computational fluid dynamics model was employed to simulate the impact of a breaking wave on the foundation of an offshore wind turbine. The accuracy of the numerical simulation was validated in comparison with published experimental results for the Large Wave Channel (GWK) at Hannover, Germany. To understand the influence of the wave-breaking location on the monopile support structure, a series of shoaling waves with different spilling and plunging breaking wave types were considered in terms of the surf-similarity parameter (ξ_0)[4] and relative breaking distance (x_b'). After processing the total wave load with an empirical mode decomposition method and a low-pass filter, the instantaneous nature of the slamming wave load generated by different breaking wave types was obtained. Subsequently, an exponential-type refined dynamic model was established to consider the characteristics of the filtered slamming wave load. ξ_0 and x_b' were found to be dominant factors for the run-up phenomena, slamming characteristics, and wave-dependent parameters. The results demonstrated that these two coefficients can be applied to determine the nature of the run-up and slamming wave loads.

Wave Conditions

The surf similarity parameter ξ_0 is used to determine the wave-breaking type. Twenty Iribarren numbers in the ranges of $\xi_0 < 0.5$ (Spilling) and $0.5 < \xi_0 < 2.3$ (Plunging) are presented in **Fig.1(a-b)** and **Fig.1(c-d)**, respectively. These wave conditions are simulated under a water depth d of 3.8 m, sloping bottom angle β of 5.71°, and cylinder axis position of 45 m from the inlet.

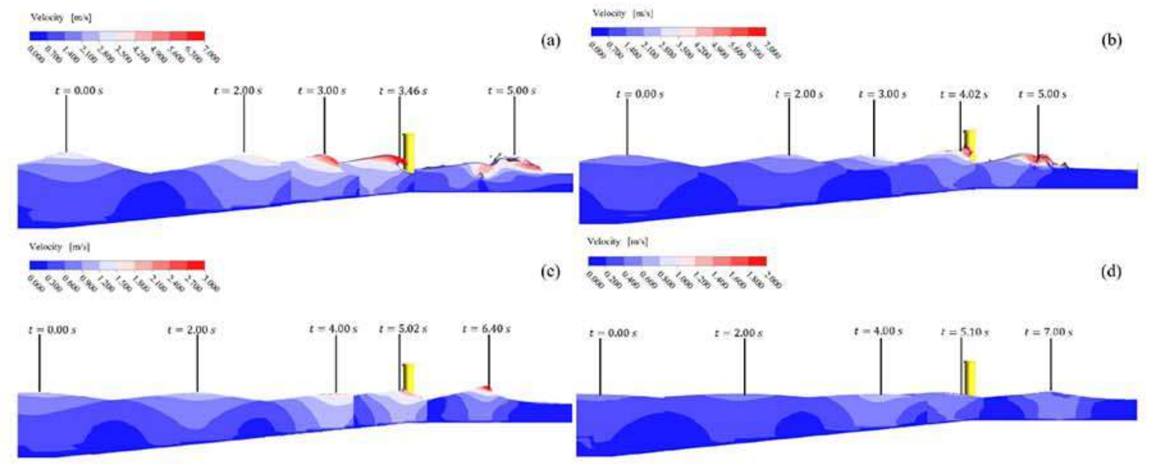

Fig.1 Scenarios of waves propagating over the sloping bottom for cases ξ_0 = (a) 0.35, (b) 0.41, (c) 0.51and (d) 0.72.

Numerical Setup

The grid resolution is a crucial factor influencing the accuracy of the calculations obtained using the VOF method[2]. The mesh is generated by refined to 0.05 m to capture the surface elevation **[Fig.2 (a)]**. A numerical beach treatment is conducted in front of the outlet boundary to reduce the numerical reflection of waves **[Fig. 2 (b)]**.

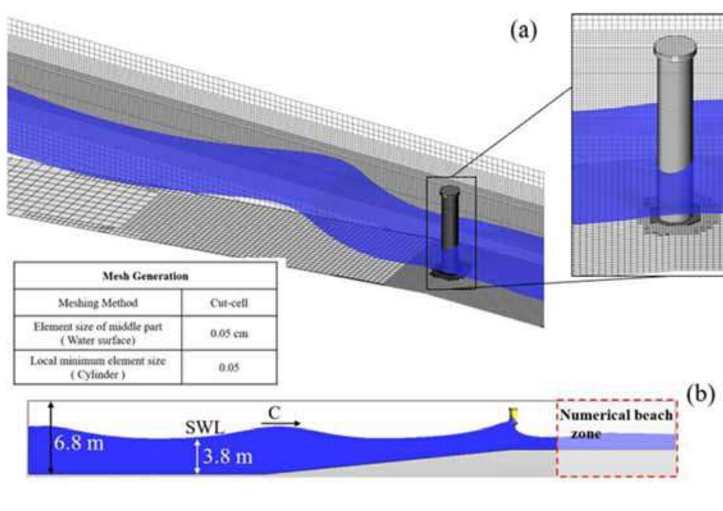

Mesh Generation	
Meshing Method	Cut-cell
Element size of middle part (Water surface)	0.05 cm
Local minimum element size (Cylinder)	0.05

Fig.2 (a) Mesh generation; and (b) numerical beach treatment.

Result and Discussion

To test the sensitivity of the CFD model to the grid size and time step, the wave conditions of $H_0 = 1.3$ m and $T_0 = 4$ s were used to evaluate the wave height at the wave-breaking point. A series of convergence tests with different combinations of grid sizes and time steps were performed with simultaneous refinement[6].

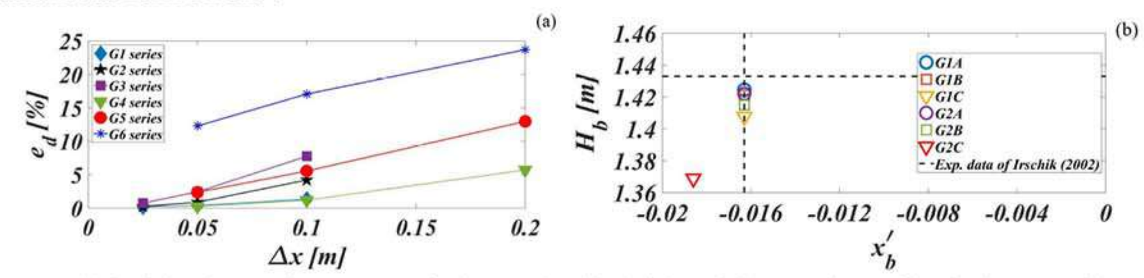

Fig. 3. (a) Spatial and temporal convergences for the wave breaking height, and (b) comparisons of the simultaneous grid and time refinement approach and the experimental data of Irschik (2002)[5].

The properties of breaking wave types for regular waves with the surf-similarity parameters ξ_0 = 0.35, 0.41, 0.51, and 0.72 are investigated to identify different scenarios and locations of wave breaking, as shown in **Fig. 1(a)-(d). Fig. 4(a)-(d)** present the refined slamming wave load model[9] with a normalized time scale for the cases of H_0= 1.8 m, 1.3 m, 0.8 m, and 0.4 m, respectively. The fitting curves were obtained by linear regression with a coefficient of determination[7, 8] (i.e., R^2 value) of 0.95. In this case, both the exponential growth and decay parameters (i.e., α_1 and α_2) can be estimated with a high confidence level.

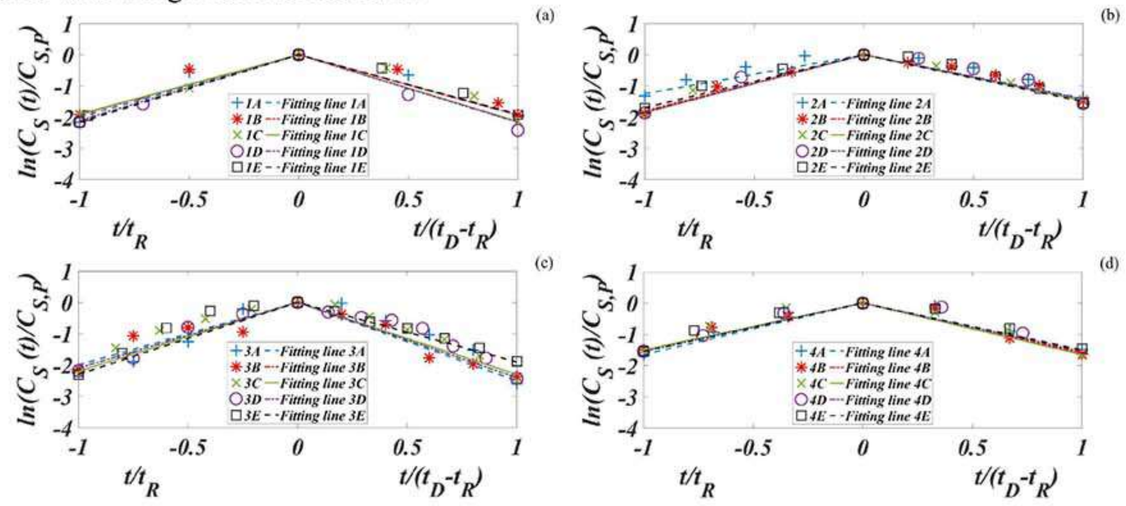

Fig.4 Refined slamming wave load models for Cases (a) H_0=1.8 m, (b) H_0=1.3 m, (c) H_0=0.8 m, and (d) H_0=0.4 m.

By mean of our CFD model, the corresponding $C_{S,P}$ and λ values with respect to x_b' are shown in **Fig. 5 (a) and (b),** respectively. Furthermore, wave-dependent parameters[9] (i.e., ω_1, ω_2, and ω_3) are presented in **Fig. 5 (c), (d) and (e),** respectively. **Fig. 5 (f)** show the normalized maximum run-up height $R_{u,max}/\eta_{max}$.

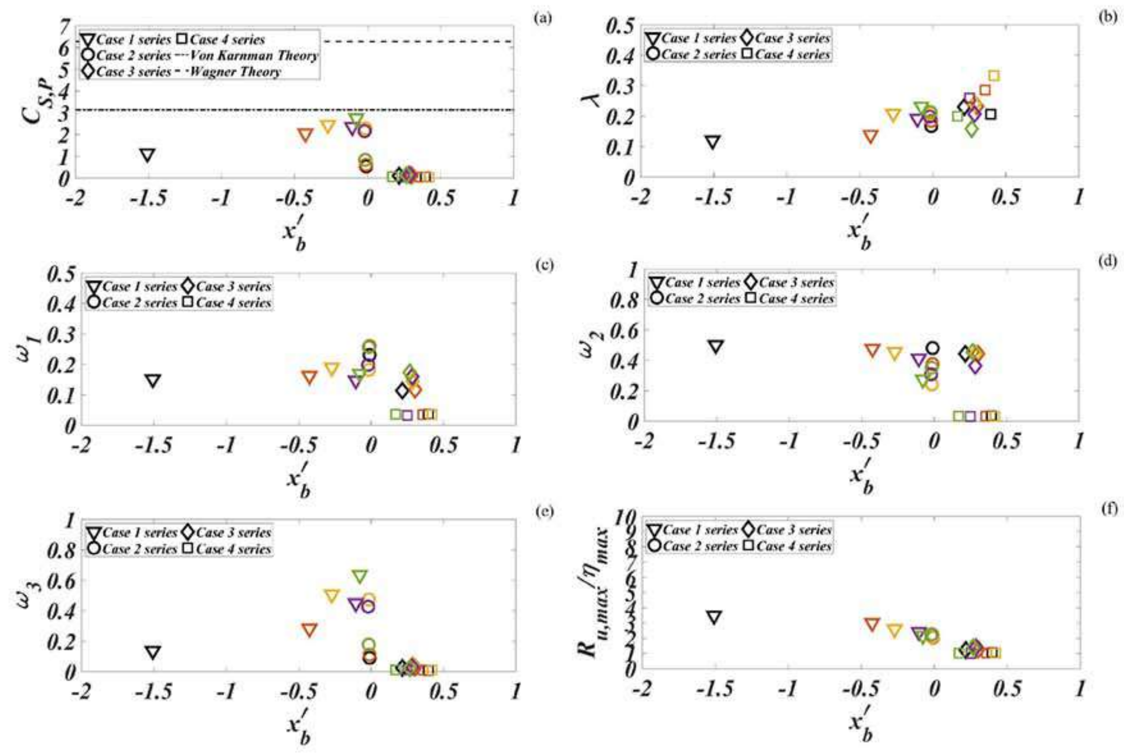

Fig.5 Variations of (a) C_S, (b) λ (c) ω_1, (d) ω_2, (e) ω_3, and (f) $R_{u,max}/\eta_{max}$ with respect to x_b'

Conclusions

1. The numerical setting of $\Delta x = 0.025$ m and $\Delta t = 0.0025$ s (i.e., $C_r = 0.5$) was in good agreement with the experimental data of Irschik [5,6] in terms of the form, load, and breaking location of the wave interacting with the monopile foundation in the wave flume.
2. According to the simulation results, the maximum slamming coefficient $C_{S,P}$ obtained from spilling breaking waves was found to approach Von Karman's value rather than Wagner's value[3]. The relative breaking distance x_b' has a considerable influence on $C_{S,P}$ and $R_{u,max}/\eta_{max}$, which have opposite trends when $x_b' < 0$. Increasing x_b' caused λ to increase and $R_{u,max}/\eta_{max}$ to decrease. The impact parameter ω_3 showed a significant response in the range of $-0.5 < x_b' < 0$ but decreased rapidly to a negligible value when $x_b' > 0$. ω_3 is dominated by $C_{S,P}$ instead of λ.

Reference

[1]ANSYS, I., ANSYS Fluent Theory Guide. Vol. 15. 2013.
[2]Vinay R. Gopala, B.G.M., Volume of Fluid Methods for Immiscible-Fluid and Free-Surface Flows. Chemical Engineering Journal, 2007. 141: p. p. 204-221.
[3]Weggel, J.R., Maximum Breaker Height. Journal Water, Harbours, and Coastal Engineering, 1972. 98: p. 529-548.
[4]Battjes, J.A. Surf Similarity. in Proceedings of 14th Coastal Engineering Conference, American Society of Civil Engineers. 1974. Copenhaguen, Denmark.
[5]Irschik, "Breaking Wave Characteristics For The Loading Of A Slender Pile" presented at the International Conference on Coastal Engineering, Cardiff, Wales, (2002)
[6]V. G. Eca L, Toxopeus S, and Hoekstra M, "Numerical Errors in Unsteady Flow Simulations", Journal of Verification, Validation, and Uncertainty Quantification **4**, p. 021001-021001 - 021001-021010. (2019).
[7]N. R. Draper and H. Smith, "*Applied regression analysis*". (John Wiley & Sons, 1998).
[8]J. L. Devore, "*Probability and Statistics for Engineering and the Sciences*". (Cengage learning, 2011).
[9]Y. Tu, Z. Cheng and M. Muskulus, "A global slamming force model for offshore wind jacket structures", Marine Structure **60**, 201-217 (2018).